A Comparison of Dipolar and Focused Inversion for EEG Source Imaging

Weinstein D.[1], **Portniaguine O.**[1], **Zhukov L.**[2]

[1]University of Utah, Salt Lake City, USA
[2]California Institute of Technology, Pasadena, USA
email: {dmw|oleg}@cs.utah.edu,zhukov@gg.caltech.edu
URL: http://www.sci.utah.edu

Introduction

Minimum norm source imaging algorithms have recently attracted considerable attention for bioelectric and biomagnetic field problems. The major advantage of source imaging over traditional dipole localization is that it does not require a priori knowledge of the number of dipole sources; it can capture both extended and multi-focal sources, independent of their mutual orientation and location. In contrast to dipole localization, the results can be consistently reproduced, as they do not depend on the seed configuration required by search algorithms [1].

It is well known that minimum norm algorithms using an L_2 norm result in overly-smoothed, distributed, shallow solutions, with most of the dipoles in the model having non-zero magnitudes. In contrast, using an L_1 norm results in strong focusing, with activity concentrated in only a few active dipoles. Unfortunately, L_1 computations are very sensitive to noise and typically do not search for a physically realistic source, but rather for the "sharpest" solution.

In investigating different norms to find a sharp, physically plausible solution, we have recently begun using Portniaguine and Zhdanov's "focusing inversion" algorithm [4]. Their method is based on re-weighted Tikhonov regularization, and has been proven to converge to the most focused solution allowed by the data. In this paper we performed current source imaging in a realistic FEM head model using both methods: iterative dipole fitting, and focusing inversion.

Method

Lead Field Matrix

The distribution of an electromagnetic field in the head is described by the linear Poisson equation:

$$\nabla \cdot (\sigma \nabla \phi) = \nabla \cdot \mathbf{J^s}, \quad \text{in } \Omega \tag{1}$$

with no-flux Neumann boundary conditions on the scalp:

$$\sigma(\nabla \phi) \cdot \mathbf{n} = 0, \quad \text{on } \Gamma_\Omega \tag{2}$$

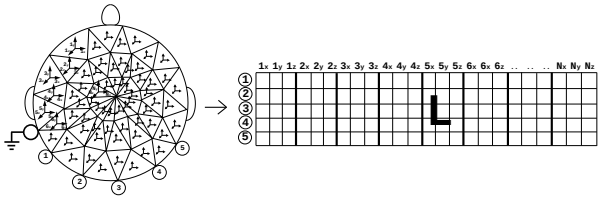

Figure 1: Depiction of the lead-field matrix. The dipole in each element corresponds to a major column of $\mathbf{L}$*, each electrode corresponds to a row of* $\mathbf{L}$*, and each entry of* $\mathbf{L}$ *corresponds to the potential measured at a particular electrode due to a particular source.*

where σ is the electrical conductivity tensor, ϕ is the electric potential, and $\mathbf{J^s}$ are the electric current sources. From the linearity of (1), it follows that the mapping from electric sources within the cranium to scalp recordings on the outside of the scalp can be represented by a linear operator $\mathbf{L}$.

The lead-field matrix, $\mathbf{L}$, defines a projection from current sources at discrete locations in the cranium to potential measurements at discrete recording sites on the scalp and is depicted graphically in Fig (1). Every entry $\bar{L}_{ij} \equiv (L^x_{ij}, L^y_{ij}, L^z_{ij})$ of the matrix corresponds to the potential that would be measured at recording site ϕ_i due specifically to dipole source $\bar{p}_j$ with components (p^x_j, p^y_j, p^z_j)

$$\phi_i = \bar{L}_{ij}\bar{p_j} = L^x_{ij}p^x_j + L^y_{ij}p^y_j + L^z_{ij}p^z_j. \tag{3}$$

A column $\bar{\mathbf{L}}_j \equiv [\bar{L}_{1,j}, \bar{L}_{2,j}, .., \bar{L}_{N,j}]^T$ of the lead field matrix projects a source $\bar{p}_j$ in the element j onto all of the electrodes. Then the total potential due to sources in all elements is given by:

$$\boldsymbol{\phi} = \bar{\mathbf{L}}_j \bar{p}_j. \tag{4}$$

The misfit between the measured data on electrodes $\boldsymbol{\phi}_i$ and the computed approximation is given by the cost function:

$$C(\bar{\mathbf{p}}) = ||\bar{\mathbf{L}}\bar{\mathbf{p}} - \boldsymbol{\phi}_\mathbf{i}||_\mathbf{2}. \tag{5}$$

This optimization problem is ill-posed and does not have a unique solution. The choice of an appropriate solution requires the application of constraints.

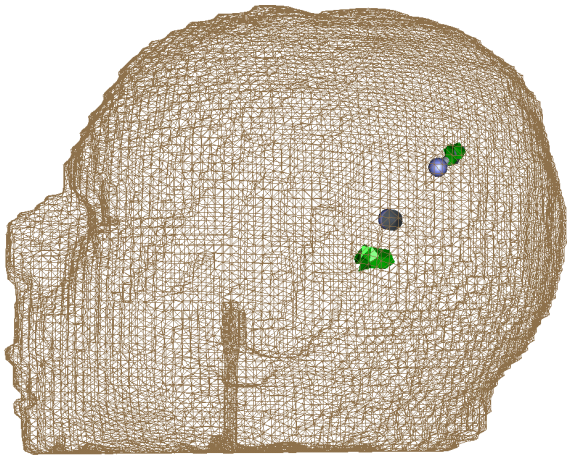

Figure 2: Isosurface of the focused inversion solution, shown with the actual dipole sources. Solution accuracy is 9 mm.

Single Dipole Source Localization

Single dipole source localization is a solution of the minimization problem (5) under the constraint that there exists only one nonzero entry $\hat{\bar{p}}_j \equiv (p_j^x, p_j^y, p_j^z)$ in the solution vector $\bar{\mathbf{p}}$, a single dipole. Since measured potentials are linear combinations of dipole components (see Eqn (3)), we can split the minimization of the problem into two parts and use a closed form, least squares solution for the dipole orientation:

$$\hat{\bar{p}}_j = (\bar{\mathbf{L}}_j^T \bar{\mathbf{L}}_j)^{-1} \bar{\mathbf{L}}_j^T \phi. \tag{6}$$

Then the cost function will explicitely depend only on the location j:

$$C(j) = ||\bar{\mathbf{L}}_j \hat{\bar{\mathbf{p}}}_j - \boldsymbol{\phi}_0||_2. \tag{7}$$

To find the global minimum of the discrete function $C(j)$, we can use either an exhaustive search over all columns of $\mathbf{L}$ or an advanced optimization algorithm, such as multi-start downhill simplex [3] or simulated annealing [2]. In our implementation, we used a multi-start simplex search.

Inverse focusing solution

An approach based on Tikhonov regularization [6] provides a general framework for the solution of ill-posed problems. It consists of the addition of a stabilizing functional to the minimization problem. This stabilizer provides additional information about the model.
Portniaguine and Zhdanov [4] have formulated a robust version of the algorithm as a minimization of a Tikhonov parametric functional that features a specially selected focusing stabilizer:

$$C(\bar{\mathbf{p}}) = ||\bar{\mathbf{L}}\bar{\mathbf{p}} - \boldsymbol{\phi_0}||^2 + \lambda \sum_j \frac{p_j^2}{p_j^2 + \beta^2} \tag{8}$$

where, as before, $\bar{p}_j$ is the j-th element of a model vector (strength of the dipole component for a corresponding voxel); $\mathbf{L}$ is the lead field (sensitivity) matrix; $\boldsymbol{\phi}_0$ is the vector of observed data; λ is the regularization parameter; and β is the damping parameter. Below we follow the numerical implementation of the algorithm described in [5].

Modeling

For our model, we constructed a tetrahedral finite element mesh (70214 nodes, 396285 elements, and 129 electrodes) from MRI data, and coregistered digitized electrode positions. This model contained different conductivity regions, corresponding to skin, bone, CSF, gray matter and white matter.

Computations

Using the above finite element model, we computed the lead field matrix relating the dipole source vector to the electrode potentials [7] and then used that matrix to drive our focusing inversion and dipole source localization methods.
To compare these methods, we simulated EEG recordings from two dipole sources located within different regions of the brain. We then performed focusing inversion and dipole fitting on the model. With focusing inversion, we were able to recover both regions of activation, within an accuracy of 9mm. A comparison of the focusing inversion solution and the true sources is shown in Fig (2). The focusing inversion solution required over an hour of CPU time to generate its solution.
In contrast, dipole fitting produced a single strong "phantom" dipole located between the two sources (15mm from one source, 30mm from the other), and a subsequent dispersed cloud of weaker correction dipoles to correct for the residual. The phantom source is shown in red in Fig (3), compared to the two true sources shown in blue. Each dipole was recovered in approximately one minute using the lead field matrix for the forward projections. The total time to compute ten iterative dipole fits (each time fitting a new dipole to best account for the residual in the system) was less than fifteen minutes.

Conclusions

We have compared a non-parameterized minimum norm solution to an iterative dipole fit solution for measurements generated from two dipoles in a realistic finite element head model. Whereas the minimum norm solution takes longer to solve, it produces significantly more accurate results. This is due to the fact that the misfit field (the field of misfit due to a single ideal dipole in each element) does not have strong minima surrounding the true sources, but rather an elongated basin be-

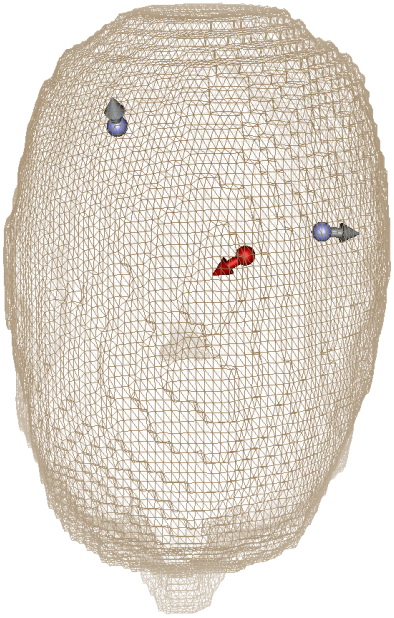

Figure 3: Fitting a single dipole source (shown in red) to a solution due to multiple dipole sources (shown in blue/gray).

tween them. As a result, the best single dipole fit is not found to be at one of the true sources, but rather between them. More research is required to better analyze the relationship between source configurations and misfit fields.

References

[1] Lutkenhoner, B., Greenblatt, R., Hamalainen, M., Mosher, J., Scherg, M., Tesche, C., and Valdes Sosa, P. Comparison Between Different Approaches to the Biomagnetic Inverse Problem: Workshop Report, Biomag96: Proceedings of the Tenth International Conference of Biomagnetism. Springer-Verlag, NY, 2000.

[2] Metropolis, N., Rosenbluth, A., Rosenbluth, R., Teller, A., and Teller, E. Equation of state calculations by fast computing machines J. Chem. Phys., 21:1087-1092, 1953.

[3] Nedler, J., and Mead, R. A simplex method for function minimization Comput. J. (UK), 7:308-313, 1965.

[4] Portniaguine, O., and Zhdanov, M.S. Focusing geophysical inversion images, Geophysics, 64:874-887, 1999.

[5] Portniaguine, O., Weinstein, D., and Johnson, C. Focusing Inversion of Electroencephalography and Magnetoencephalography 3rd Noninvasive Symposium on Noninvasive Functional Source Imaging, 2001.

[6] Tikhonov, A.N., and Arsenin, Y.V. Solution of ill-posed problems, Winston and Sons, 1977.

[7] Weinstein, D., Zhukov, L., and Johnson, C. Lead-field bases for electroencephalography source imaging, Ann. Biomed. Eng., 28:1-7, 2000.

Acknowledgments

This work was supported by the National Institutes of Health, National Center for Research Resources, grant number 1-P41-RR12553-2.